Radiology

CT in Transcatheter Aortic Valve Replacement[1]

Philipp Blanke, MD[2]
U. Joseph Schoepf, MD
Jonathon A. Leipsic, MD

Transcatheter aortic valve replacement is a new method to treat patients with symptomatic, severe aortic stenosis who are at high surgical risk. Short- and midterm results have been encouraging, with more than 90 000 procedures performed worldwide. Patient selection, prosthesis sizing, and access strategies heavily rely on noninvasive imaging. Computed tomographic (CT) angiography is increasingly used for peri-interventional evaluation, as this modality allows for objective three-dimensional assessment of the aortic root, evaluation of the iliofemoral access route, and prediction of appropriate projection angles for prosthesis deployment. Compared with two-dimensional imaging techniques, CT provides comprehensive information about aortic annulus anatomy and geometry, supporting appropriate patient selection and prosthesis sizing. Recently, integration of CT measurements into sizing algorithms has been demonstrated to significantly reduce the incidence of paravalvular regurgitation, compared with prosthesis sizing with two-dimensional echocardiography. In addition, CT-based vascular access planning has been shown to reduce vascular access complications. Postprocedural CT imaging allows for the documentation of procedural success, evaluation of prosthesis positioning, and identification of asymptomatic complications. In this article, the rapidly emerging role of CT in the context of transcatheter aortic valve replacement will be described.

Supplemental material: *http://radiology.rsna.org/lookup/suppl/10.1148/radiol.13120696/-/DC1*

[1] From the Department of Radiology and Radiological Science and Division of Cardiology, Department of Medicine, Medical University of South Carolina, Ashley River Tower, MSC 226, 25 Courtenay Dr, Charleston, SC 29425 (P.B., U.J.S.); and Department of Radiology and Division of Cardiology, Department of Medicine, University of British Columbia, Vancouver, BC, Canada (J.A.L.).
Received March 24, 2012; revision requested May 14; final revision received July 21; final version accepted August 28.
Address correspondence to U.J.S. (e-mail: *schoepf@musc.edu*).

[2] **Current address:** Department of Diagnostic and Interventional Radiology, University Hospital Würzburg, Würzburg, Germany.

Aortic stenosis is the most prevalent cardiac valvular disease in the Western world (1,2). Aortic valve replacement is indicated for symptomatic patients with severe aortic stenosis, because the prognosis for untreated patients is poor (3). Surgical valve replacement is the definitive treatment for severe aortic stenosis and is technically possible in patients of any age (3,4). However, as many as 30% of patients with aortic stenosis are not considered surgical candidates because of comorbidities and estimated extreme surgical mortality risk (5). Transcatheter aortic valve replacement (TAVR, also referred to as transcatheter aortic valve implantation, or TAVI) is a recently introduced method to treat selected high-risk patients with aortic stenosis (6–8). As of mid-2013, more than 90 000 procedures have been performed worldwide (9), mostly in patients at high surgical risk. Safety, efficacy, and noninferiority to conventional open surgery have been demonstrated in recent prospective multicenter investigations (10,11).

Essentials

- CT allows for simultaneous assessment of the aortic root and iliofemoral morphology, thereby providing relevant information for determining patient eligibility, access strategy, and prosthesis selection in transcatheter aortic valve replacement.
- As a three-dimensional (3D) imaging modality, CT enables assessment of the aortic annulus in its true plane, allowing 3D assessment of annular geometry and dimensions; CT thus enables refined prosthesis sizing with a lower incidence of paravalvular regurgitation compared with prosthesis sizing with two-dimensional echocardiography.
- Extraction of aortic root geometry from CT data can aid in the prediction of suitable procedural projection angles and thus enhance procedural success and efficiency.
- CT angiography of the iliofemoral vasculature enables evaluation of vessel tortuosity, calcifications, and vessel diameters and may thereby inform decisions on the most suitable interventional approach.
- Postprocedural CT imaging allows for the documentation of procedural success, evaluation of prosthesis positioning, and identification of asymptomatic complications.

Prior to TAVR, patients undergo an extensive work-up to assess aortic root anatomy and the coronary and iliofemoral arteries. This evaluation is essential to determine patient eligibility and to ultimately guide procedure planning. Traditional diagnostic modalities used in the evaluation include echocardiography, cardiac catheterization, and, in the case of a transfemoral approach, aortoiliac angiography (12). The results of these diagnostic studies are used to determine the procedure's feasibility, to select the access strategy, and for transcatheter heart valve (THV) sizing. The ability of computed tomography (CT) to comprehensively address all relevant aspects in the work-up for TAVR is increasingly recognized. Accordingly, CT has become increasingly relied on in a number of centers for the evaluation of the aortic annulus, the root, and the iliofemoral anatomy, with ever-growing evidence that integration of CT into TAVR planning actually reduces procedural complications, such as paravalvular regurgitation (13). In this article we describe the rapidly emerging role of CT for aortic root assessment, CT-based THV sizing, iliofemoral assessment, and postprocedural imaging in the context of TAVR.

Procedural Overview

Two THV systems have seen wide clinical application: the balloon-expandable Edwards SAPIEN and SAPIEN XT valves (Edwards Lifesciences, Irvine, Calif; SAPIEN XT is currently not available in the United States) and the self-expandable CoreValve ReValving System (Medtronic, Minneapolis, Minn; not currently available in the United States) (Fig 1) (6–8,14). Further systems have recently received CE Mark or Conformité Européenne Mark certification in Europe, such as the JenaValve (JenaValve Technology, Munich, Germany) and the Direct Flow Medical Transcatheter Aortic Valve System (Direct Flow Medical, Santa Rosa, Calif). Other dedicated systems are on the verge of becoming clinically available. However, due to space limitations, we focus on the two most prevalent systems.

In general, access to the native valve can be achieved by using a retrograde transarterial technique, typically via the femoral or subclavian arteries. Alternatively, an anterograde approach with a transapical technique can be used by cannulation of the cardiac apex, although this route is not available for self-expanding THVs. THV deployment is now most commonly preceded by balloon aortic valvuloplasty to facilitate the passage of the THV through the stenotic native aortic valve. Subsequently, the unexpanded valve is appropriately positioned within the native aortic valve annulus with fluoroscopic and often transesophageal echocardiographic guidance. The SAPIEN and SAPIEN XT valves are expanded by a balloon during burst ventricular pacing to minimize cardiac output and to prevent migration of the valve during deployment. The CoreValve is self-expanding and is generally deployed without pacing. Achieving optimal positioning of the transcatheter aortic prosthesis is of great importance to

Published online
10.1148/radiol.13120696 **Content codes:** CA VA CT

Radiology 2013; 269:650–669

Abbreviations:
ECG = electrocardiography
PARTNER = placement of aortic transcatheter valve
3D = three-dimensional
TAVR = transcatheter aortic valve replacement
TEE = transesophageal echocardiography
THV = transcatheter heart valve

Conflicts of interest are listed at the end of this article.

Figure 1

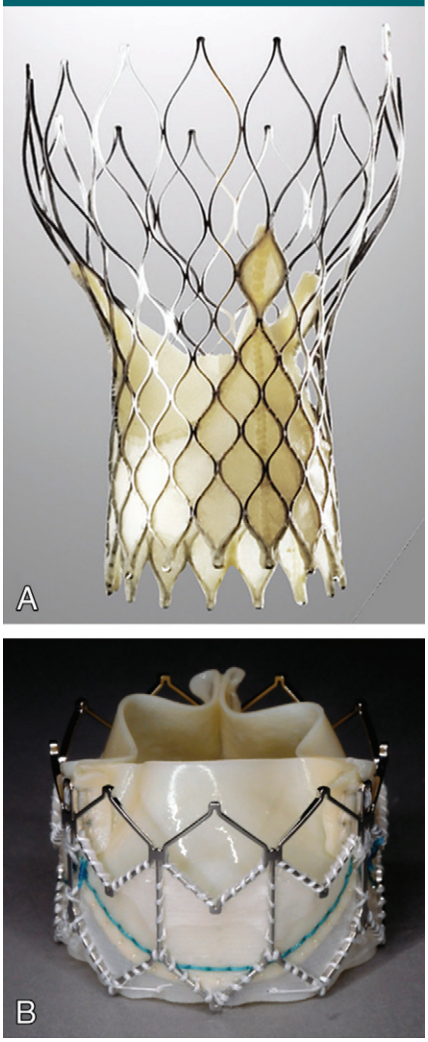

Figure 1: *A,* Self-expanding Medtronic CoreValve composed of a nitinol stentframe and porcine pericardial leaflets. *B,* Balloon-expandable Edwards SAPIEN XT composed of a cobalt-chromium stentframe with bovine pericardial leaflets.

the procedural success, as the goal is to displace the native valve cusps and deploy the device within the native valve annulus. If the valve is deployed too low, there is an increased risk of heart block, paravalvular regurgitation, and mitral valve dysfunction (15). Alternatively, if the valve is positioned too high, there is increased risk of valve embolization into the aorta, paravalvular regurgitation, and aortic root injury (15).

Evidence Base: Trials of TAVR and Review of Current Data

As of mid-2013, multiple single and multicenter trials and registries have documented favorable outcomes by using a wide spectrum of endpoints, including survival, symptom status, quality of life, and the need for repeat hospitalization. However, to date, PARTNER (Placement of aortic transcatheter valve) A and B are the only two randomized trials evaluating TAVR in high-risk surgical and extremely-high-risk nonsurgical population (10,11). In PARTNER B, 358 patients with severe aortic stenosis who were deemed at excessively high risk for conventional surgery were randomized to medical treatment (including balloon aortic valvuloplasty) versus transfemoral balloon-expandable TAVR (10). PARTNER B showed a 20% absolute reduction in 1-year all-cause mortality in the TAVR cohort, compared with the standard of care (30.7% vs 50.7%). In PARTNER A, 699 high-risk but still operable patients with symptomatic, severe aortic stenosis were randomized to either TAVR (transfemoral or transapical) or conventional surgery (11). In this trial, TAVR was noninferior to surgical aortic valve replacement for all-cause mortality at 1 year (24.2% vs 26.8%) and at 2 years (33.9% vs 35.0%) (16).

While PARTNER B defined a new treatment option by documenting the superiority of transfemoral TAVR to conservative therapy in otherwise not operable patients, PARTNER A established that TAVR constitutes an acceptable alternative to conventional surgery in selected high-risk, but still operable patients (10,11). One-year mortality rates in the nonrandomized European registry for the SAPIEN XT device were 18.9% for the transfemoral approach and 27.9% for the transapical approach, as patients treated transapically had a higher perioperative mortality due to the more severe comorbidities in this cohort (17). For the CoreValve device, survival data are limited to single center and multicenter registries, as data from randomized trials, such as the currently ongoing Medtronic CoreValve U.S. Pivotal Trial, is not yet available (18). In the Italian registry, 1-year mortality was 23.6% (19).

Major concerns that remain with TAVR are paravalvular regurgitation, vascular complications, and stroke. Paravalvular regurgitation, as diagnosed with postdeployment echocardiography, is usually categorized as trivial, mild, moderate, or severe (20). Moderate to severe paravalvular regurgitation was observed in 12.9% and 6.8% of TAVR patients at 30 days and 1 year, respectively, in PARTNER A, compared with 0.9% and 1.8%, respectively, in the surgical arm (11). In PARTNER B, moderate or severe paravalvular regurgitation was present in 11.8% of patients at 30 days and in 10.5% at 1 year (10). Importantly, paravalvular regurgitation has shown an association with increased in-hospital (21) and midterm mortality, as is clearly demonstrated by the 2-year outcome data from the PARTNER A cohort (16). Most important, even mild paravalvular regurgitation was associated with increased late mortality (16,22). Current data on vascular complications are discussed below.

Aortic Root Anatomy and THV Characteristics

The aortic root is the direct continuation of the left ventricular outflow tract and extends from the basal attachment of the aortic valve cusps within the left ventricle to their peripheral attachment at the level of the sinotubular junction. The root is widest at the midpoints of the sinus and narrowest at the basal attachment of the leaflets and the sinotubular junction (23). The semilunar leaflet insertions take the course of a three-pronged coronet rather than forming a ring as implied by the term *annulus*. The base of the crown can, however, be thought of as a virtual plane, formed by the most basal attachment points of the three cusps (Fig 2) (23,24). Although the anatomic configuration of the annulus has been extensively described, insights into the in

Figure 2

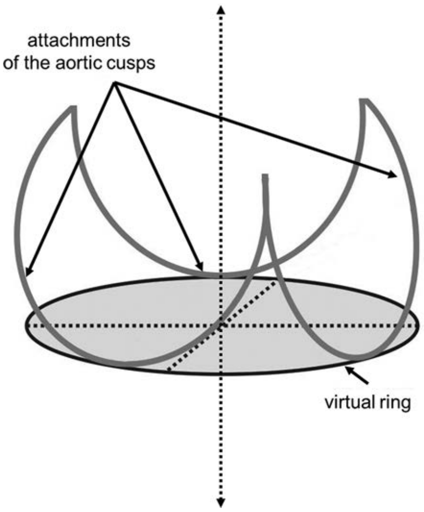

Figure 2: Schematic of the aortic valvular complex and the virtual ring approach of the aortic annulus. Semilunar hinges of the aortic cusps form a three-pronged coronet. Most basal attachment sites are connected by the virtual ring, encircling the cross-sectional area of the aortic annulus and defining its true plane.

Table 1

Valve Size, Introducer Profile, and Required Vessel Diameter

Device	Introducer Profile	Outer Sheath Dimensions	Required Vessel Diameter (mm)
Edwards SAPIEN THV with RetroFlex 3 Delivery System			
23 mm	22F	25F (8.4 mm)	≥ 7
26 mm	24F	28F (9.2 mm)	≥ 8
Edwards SAPIEN XT THV with NovaFlex+ Delivery System and eSheath*			
23 mm	16F	20F (6.7 mm)	≥ 6
26 mm	18F	21F (7.2 mm)	≥ 6.5
29 mm	20F	27F (9 mm)	≥ 7
CoreValve ReValving System			
26 mm	18F	Depend on sheath used	≥ 6
29 mm	18F	Depend on sheath used	≥ 6
31 mm	18F	Depend on sheath used	≥ 6

Note.— Edwards SAPIEN XT THV and CoreValve ReValving System are not approved in the United States.

* Expandable introducer sheath. The reported values are for the unexpanded state.

vivo anatomy of the aortic valvular complex, which cannot be obtained from surgical or pathologic inspection of a nonbeating heart, only became possible with modern three-dimensional (3D) imaging techniques (25). In vivo, the aortic annulus has been shown to be of a noncircular, often oval shape at both 3D transesophageal echocardiography (TEE) and CT (25–27). As a result, it does not lend itself to evaluation with a two-dimensional imaging technique. Furthermore, the aortic root is a dynamic structure, with the aortic annulus not only subject to pulsatile changes, but also to contour deformity related to the movement of the aorto-mitral junction or changing volume and pressure in the left atrium (28,29). Subsequent changes in geometry and dimension have to be considered but historically have been largely ignored or underappreciated.

Although a number of THV designs are in development and clinical test phases, our discussion focuses on the two most commonly used, clinically available THV platforms (Table 1). These two devices follow different design principles. The balloon-expandable second-generation SAPIEN, available in 23- and 26-mm diameters, consists of a trileaflet bovine pericardial valve sewn into a tubular stainless steel stent of 14–16 mm in length. The third-generation SAPIEN XT THV (23, 26, and 29 mm; 14–19 mm in length) utilizes a redesigned cobalt chromium alloy frame with thinner struts, enabling deployment by a lower profile delivery system. A 20-mm transfemoral SAPIEN XT model has been utilized in Canada and Japan (14,30), a transapical 29-mm THV is available in Canada and Europe, and a transfemoral version of the 29-mm THV has recently been approved in Europe. The lower two-thirds of the struts are covered by a sealing cuff. The device is properly positioned if the THV inflow is located below the native annulus plane as the single point of fixation. The reported diameters are nominal diameters reached at both the ventricular and aortic ending when fully expanded by the balloon.

The CoreValve THV consists of a trileaflet porcine pericardial valve mounted on a self-expanding nitinol frame, which is markedly longer (53–55 mm) than the balloon-expandable THV, as the unfolded prosthesis extends into the ascending aorta. The manufacturer refers to its valve as supra-annular, as the valve leaflets are mounted approximately 12 mm above the ventricular end and are thus 2–7 mm above the native annular plane. When correctly positioned with the ventricular end in an intra-annular position 5–10 mm below the bottom of the native noncoronary cusp, device migration is mainly prevented by radial force at the in-flow level, while the larger ascending aortic end predominantly aids proper device orientation and, to a lesser degree, device fixation. Intra-annular implantation and a sealing skirt mitigate paravalvular regurgitation. A constrained zone in the mid-portion prevents occlusion of the coronary ostia. The CoreValve THV is available in nominal 26-, 29-, and 31-mm diameters for annulus sizes of 20–29 mm wit echocardiography, all mounted into an 18-F delivery system. Importantly, the nominal device diameter refers to the diameter at the ventricular end, not to the actual valve diameter.

Preprocedural Assessment: CT Angiographic Technique and Protocols

When CT is integrated into the TAVR work-up, acquisition protocols have to address the following challenges: *(a)* provide motion-free images of the aortic root at specific time-points within the cardiac cycle by means of electrocardiographic (ECG) synchronization, *(b)* compensate for arrhythmia such as atrial fibrillation, *(c)* long z-axis coverage to visualize the entire aorta including the proximal supra-aortic vessels and iliofemoral axis, and *(d)* minimize contrast media volumes in the setting of impaired renal function.

The largest dimensions of the aortic annulus are ordinarily found during systole (31). Thus, in analogy to traditional echocardiographic assessment, ECG-synchronized data acquisition should aim at covering the entire systolic cardiac phase. At our institutions, we therefore prefer retrospectively ECG-gated synchronization with high tube current settings common to routine cardiac CT protocols and rather wide pulsing windows. This incurs higher radiation dose but allows for more latitude in image reconstruction for assessment of the annulus, which takes precedence over radiation dose reduction in this elderly population who frequently have atrial fibrillation (32). A more relevant disadvantage of retrospectively ECG-gated techniques consists in relatively long scan times, requiring higher contrast media volumes. ECG-gated image acquisition should cover at least the aortic root, preferably the entire heart. Most often, the ECG-synchronized data acquisition is then followed by a subsequent non–ECG-synchronized CT angiographic study of the chest, abdomen, and pelvis for simultaneous assessment of the access route. This latter scan should extend from the proximal supra-aortic vessels (or the entire subclavian arteries if this access route is an option) and extend caudally to below the femoral heads so as to fully visualize the common femoral artery access site.

Given the nature of the underlying disease, in our practice we do not administer additional β-blockers prior to CT to achieve lower heart rates. β-blockers may depress left ventricular systolic function and thereby worsen symptoms caused by critical aortic stenosis. In addition, fast heart rates usually do not interfere with aortic root assessment to the same extent as with dedicated CT coronary artery evaluation.

TAVR Evaluation in Patients with Impaired Renal Function

Currently, patients who are considered for TAVR are ordinarily in a multimorbid state and/or of advanced age, making them ineligible for a traditional surgical approach. While this fact minimizes possible concerns over radiation exposure, it is associated with a high prevalence of renal disease. In fact, recent single-center data from the German Heart Center (33) stated that 18% of patients undergoing TAVR had impaired renal function. Although the risk of permanent renal adverse effects after intravenous contrast media administration is less well studied than that after intra-arterial injection, the prevention of further renal deterioration should be one of the priorities when planning a CT examination in the context of TAVR. Different approaches to reduce contrast media volumes currently exist. The sole use of high-pitch scanning protocols targeting the systolic phase of the cardiac cycle at the level of the aortic root has been reported (34), without a preceding ECG-gated acquisition of the aortic root and/or heart. However, while this latter approach may enable a decrease in the total volume of contrast medium to 40 mL due to very short acquisition times, it does not allow for dynamic assessment of the aortic root and may be of limited use in patients with atrial fibrillation (34). In our experience, to reliably perform root measurements, the intraluminal contrast medium attenuation in the left ventricular outflow tract and the aortic root can be lower than is desired for coronary CT angiography. We routinely reduce the contrast medium volume to as little as 30 mL, which allows for sufficient visualization of the aortic root if coverage of retrospectively ECG-gated CT data acquisition is limited to this anatomic structure. Evaluation of the iliofemoral vasculature is then performed by subsequent high-pitch data acquisition by using the same contrast medium bolus, if this technique is available. Alternatively, nonenhanced data acquisition of the abdomen and pelvis may allow for assessment of anatomy and calcifications (9). In cases of severe renal dysfunction, direct intra-arterial contrast media injection for iliofemoral CT angiography may be helpful. For this purpose, injection of less than 15 mL of contrast media has been reported to be sufficient (35,36). Finally, in patients with borderline renal function, we avoid performing CT angiography and the invasive angiography the same day.

Aortic Annulus Measurement with CT

Because of the isotropic nature of image data acquired with current CT systems, the aortic annulus can be assessed in its true plane immediately below the hinge point of the aortic valve cusps (Figs 2, 3; Movie 1 [online]). Most commonly, the long axis (maximum) and the short axis (minimum) are then measured, allowing for the calculation of a mean diameter. Planimetry can also be performed, enabling both perimeter and area measurements; derived diameters can be calculated on the basis of the formula for the area of a circle or the perimeter of a circle, respectively (37).

CT measurements have been shown to be highly reproducible at both inter- and intrareader correlation (32,38). The aortic root compliance and deformation during the cardiac cycle result in cross-sectional area and diameter changes (Fig 4). Most interestingly, two components affect cross-sectional geometry: Stretch of the confining anatomic structures leads to a simultaneous increase in area and perimeter during systole (31). However, flattening

Figure 3

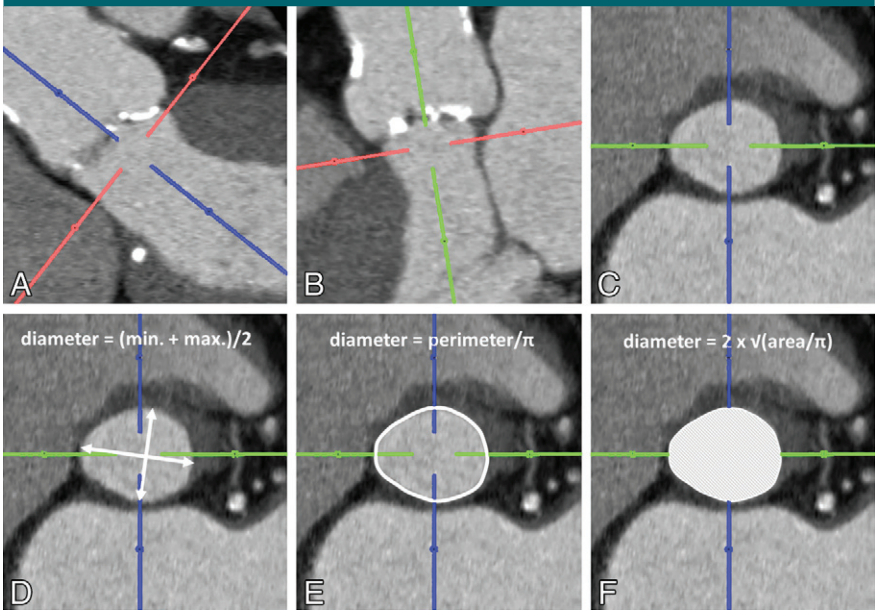

Figure 3: Contrast-enhanced retrospectively ECG-gated data set in a TAVR candidate. *A,* Coronal oblique and, *B,* sagittal oblique views are adjusted so that the resulting, *C,* double-oblique transverse view transects through the most basal attachment points of all three cusps, defining the true annulus plane (virtual ring). Annulus dimensions can be evaluated by assessing minimum *(min.)* and maximum *(max.)* diameters with, *D,* subsequent averaging, *E,* planimetrically based on perimeter or, *F,* cross-sectional area followed by calculation of derived diameters.

Figure 4

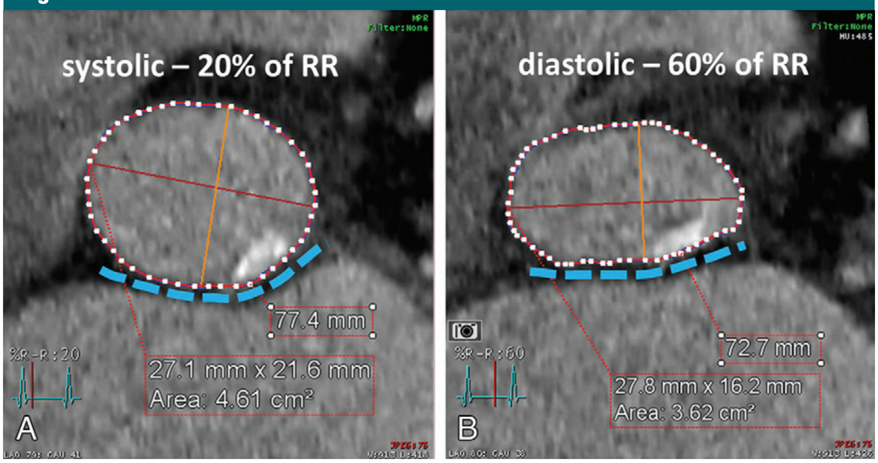

Figure 4: Contrast-enhanced retrospectively ECG-gated data set in a TAVR candidate with severe aortic stenosis. *A,* Midsystolic and *B,* early-diastolic double-oblique transverse views transecting through the annulus plane at the most basal attachments of all three cusps. Pulsatile changes lead to an increase in perimeter and cross-sectional area during systole. Conformational geometrical changes are predominantly due to bulging and flattening of the aorto-mitral junction (dashed line) during systole and diastole with subsequent increase in eccentricity during diastole.

of the aortic-mitral junction during diastole with subsequent shortening of short-axis dimensions leads to an increase in eccentricity with a greater than proportional decrease in area compared with perimeter. Although recent investigations first suggested that changes in perimeter are negligible in patients with severe aortic stenosis (28), we found an average 18.2% ± 6.1 (standard deviation) relative difference between maximum and minimum cross-sectional area and an average 7.3% ± 2.1 difference between maximum and minimum perimeter measurements (31). This translates into differences in derived average diameters of 8.7% ± 2.8 and 7.3% ± 2.1, respectively (31), which has implications for correct THV sizing (see below). Largest dimensions are most commonly observed at 20% of the R-R interval (31).

Aortic Annular Geometry and THV Sizing: Evolving Role of CT

Current implantable valves are designed for specific annular sizes. Unlike during surgical aortic valve replacement, where prosthesis sizing is performed by using a sizing probe with the benefit of direct visualization, TAVR relies exclusively on pre-and periprocedural imaging for valve selection. Annular measurements have historically been performed by using two-dimensional transthoracic echocardiography, TEE, or calibrated aortic angiography; however, discordance between measurements obtained with these two-dimensional techniques has been reported (39–41). Compared with calibrated aortic angiography, transthoracic echocardiography systematically underestimates annulus dimensions by 1.5 mm ± 2.3 (41), while there is no relevant systematic difference between transthoracic echocardiography and TEE (40). The limitations of two-dimensional measurement techniques mainly arise from the noncircular configuration of the annulus (25, 26, 38–40, 42–45) described above. There has been growing interest in better defining the shape, geometry, and size of the aortic root complex through the integration of 3D imaging techniques such as CT, magnetic resonance (MR) imaging, and 3D TEE (25,46). The noncircular, ovoid, at times elliptical, nature of the annulus is reflected by significant differences, of 5.5 mm on average, between the short and long axis, based on CT findings (45). It is well established that comprehensive CT-based determination of area- or perimeter-derived diameters or mean diameter (average of short and long axis) typically results in measurements that exceed those obtained with echocardiography. Two-dimensional echocardiographic measurements usually transect the annulus close to its short axis. This systematic difference amounts to 1.1–1.5 mm for TEE (27,38) and 1.3 mm for transthoracic echocardiography (41), compared with that for CT. Similarly, annular assessment with 3D TEE has reported larger annular sizes than those observed by using traditional two-dimensional TEE (25). Because of its eccentric shape, the perimeter-derived diameter will always exceed both the area-derived diameter and the mean diameter according to short- and long-axis measurements (31,37).

Although CT is rapidly emerging as an attractive, comprehensive modality in the work-up for TAVR, current recommendations, clinical practice, and currently available randomized trial data (10,11) are solely based on echocardiographic measurements of the annulus. Accordingly, patient eligibility for TAVR and THV sizing are largely determined on the basis of aortic annulus measurements at transthoracic echocardiography and TEE. Clinical outcomes with TEE-based annulus measurements and routine oversizing of the valve by 1–2 mm in regard to the TEE-based annulus diameter have been satisfactory; however, there remain approximately 10%–15% of patients who develop postprocedural moderate to severe paravalvular regurgitation (10,11). There is hope that annular measurements acquired by using 3D imaging techniques, such as TEE and CT, will provide a more granular assessment of the aortic root and annular geometry and eccentricity to allow for more accurate sizing and thus reduce the rate of paravalvular regurgitation (39,45), further improving on these outcomes. As of mid-2013, numerous retrospective analyses have demonstrated that 3D measurements of the annulus at multidetector CT can identify patients who will experience greater than mild paravalvular regurgitation (45,47,48). Interestingly, this discriminatory capability was demonstrated to be superior to the discriminatory capability of TEE (49). Importantly, these CT annular measurements have recently been shown to help reduce the incidence of greater than mild paravalvular regurgitation in a prospective, multicenter study, where the integration of CT into THV sizing reduced greater than mild paravalvular regurgitation from 12.8% in a historical control group to 5.3% (13).

However, at present there are specific annular size limitations for TAVR based on echocardiographic measures of the annulus. For the Edwards SAPIEN valve, the annulus must measure between 18 and 27 mm (18–22 mm for 23-mm THV, 21–25 mm for 26-mm THV, 25–27 mm for 29-mm THV). For the current generation of the CoreValve device, the annulus size must range between 20 and 29 mm (20–23 mm for 26-mm THV, 23–27 mm for 29-mm THV, 26–29 mm for 31-mm THV). The rapidly increasing variety of THV models has been driving the need for more accurate annulus determination.

Proposed CT Sizing Guidelines

The development of CT-based sizing guidelines is a process in evolution. So far, this process has largely used retrospective analyses of cohorts with and without paravalvular regurgitation in an attempt to better understand appropriate THV sizing. There is evidence that oversizing is inversely related to paravalvular regurgitation. It has been shown that CT modifies THV sizing strategies in 40%–44% of patients by using a mean of the short and long axis of the basal ring when compared with THV selection with TEE (38,40). However, given the satisfactory success of the procedure so far, the suggestion of altering the sizing approach in 40%–44% of cases has largely been rejected by the TAVR community. This is almost certainly appropriate given the fact that at present, the only randomized data documenting the efficacy of TAVR is based on echocardiographic sizing of the annulus (10,11). However, CT with its isotropic spatial resolution and 3D imaging capabilities should add incremental information to two-dimensional echocardiographic assessment. While these measurements have not been validated or integrated in randomized trials, they have already proved to be helpful in predicting complications of THV undersizing, such as paravalvular regurgitation (13,45,47) or contained aortic root rupture, with aggressive THV oversizing and landing zone calcification (50,51).

For CT measures of the aortic annulus to move beyond mere additive information, a CT-based sizing scale must be integrated into THV selection. We propose a sizing scale based on both the mean of the short and long axis of the basal ring and the area measurement of the basal ring (Table 2). To minimize the risk of significant paravalvular regurgitation, the implanted THV size should be greater than the 3D area of the annulus at CT. In a recent analysis of our cohort, for THVs that were oversized by at least 10% of the annular area, there were no cases of significant paravalvular regurgitation (45). Intentional oversizing may come at a potential cost of coronary occlusion or annular rupture. However, this has not been our experience, with a historical unintentional oversizing of the area of the basal ring by approximately 5% on the basis of echocardiographic THV selection during the past 125 cases (45), where no incident of coronary occlusion or of annular injury occurred. Recently, 10%–25% oversizing of the perimeter of the aortic annulus at CT has been proposed as optimal for TAVR (52). The appeal of perimeter-based sizing is also likely to grow as recently published data sug-

Table 2

Proposed CT Sizing Criteria for Balloon-expandable TAVR

Nominal THV Diameter (mm)	External THV Area (cm^2)	Mean Diameter (mm)	Annulus Area Measurement (cm^2)	Relative Oversizing by Diameter (%)	Relative Oversizing by Area (%)
23	4.15	20–22	3.10–4.10	4.5–15	1–33
26	5.31	<25	<5.2	1–18	2–30
29*	6.61	<28.5	<6.6	1–16	0–27

* Currently not available in the United States.

Figure 5

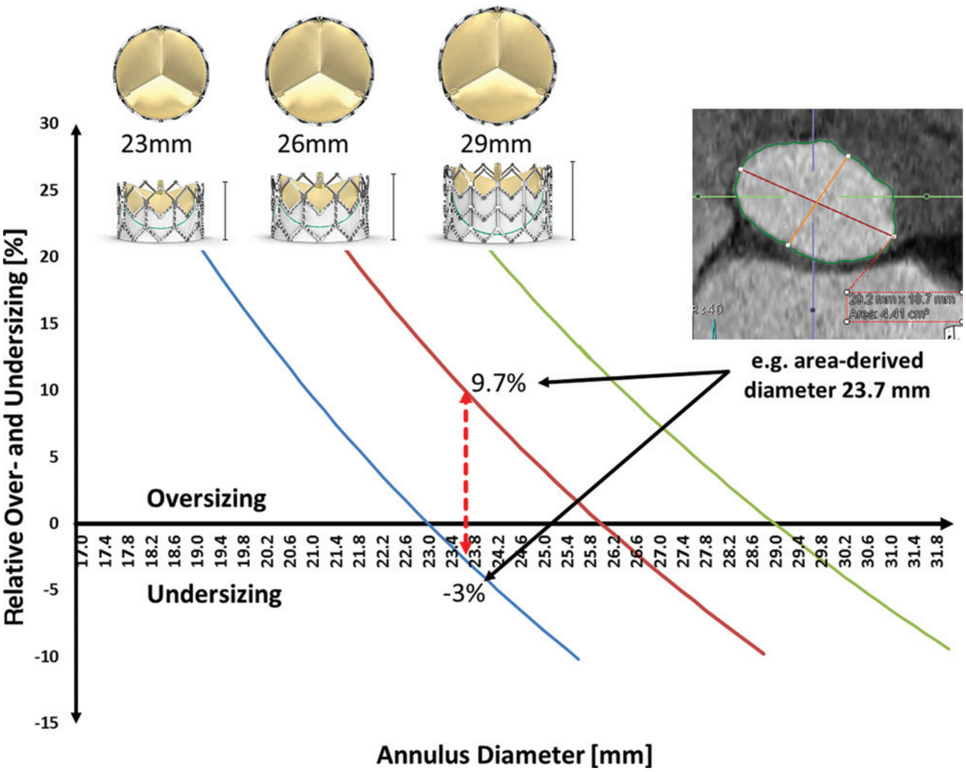

Figure 5: Illustration of relative over- and undersizing as a function of annulus diameter (An_{diam}) and selected THV size (THV_{diam}) for balloon-expandable TAVR, with nominal THV sizes of 23 mm (blue curve), 26 mm (red curve), and 29 mm (green curve). Relative over- or undersizing ($Relative_{over\text{-}under}$ [%]) is calculated as follows: $Relative_{over\text{-}under}$ (%) $= (1 - \text{nominal } THV_{diam}\ [mm]/An_{diam}\ [mm]) \times 100$. For an area-derived annulus diameter of 23.7 mm, selection of a 23- or 26-mm THV would result in 3% undersizing or 10% oversizing, respectively (dashed red line). Calculation of relative over- or undersizing can be applied to effective diameter and also to area or perimeter.

gest that the perimeter may, in fact, be the most consistent measure throughout the cardiac cycle (28).

The practical application of current CT experience remains somewhat limited at present owing to the restricted variety in valve sizes. Imagers and interventionists alike should understand and consider the potential implications of CT-based sizing and the increase in THV area when moving from the smaller to larger THVs. For the Edwards balloon-expandable valve, upsizing from a 23- to a 26-mm balloon-expandable THV is associated with an exponential 28% increase in external valve area; upsizing from a 26- to a 29-mm valve is associated with a further 25% increase (Table 2). These rather large incremental changes in THV area make it difficult to appropriately size borderline cases (Fig 5). For example, in the case of a mean 23.5-mm basal ring with an area of 4.45 cm^2, the annu-

Figure 6

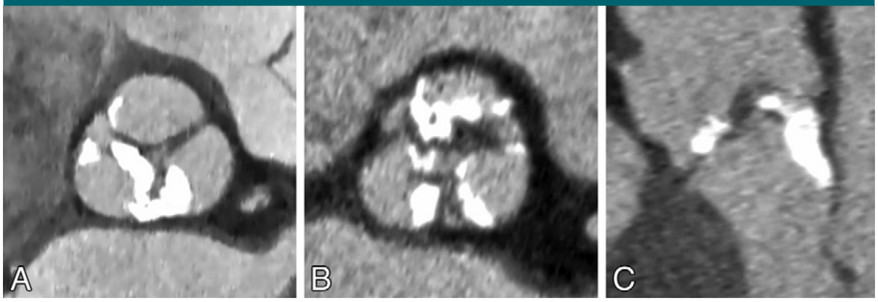

Figure 6: Contrast-enhanced retrospectively ECG-gated data sets in two TAVR candidates. Transverse oblique maximum intensity projections of the aortic valve for evaluation of calcification burden show, *A*, asymmetric and, *B*, symmetric calcifications of all three cusps. *C*, Sagittal oblique view shows that calcifications extend into the left ventricular outflow tract.

lus would appear too large for a 23-mm THV, with a high risk of paravalvular regurgitation; however, 26-mm prosthesis would result in more than 20% oversizing, which may be unacceptable. This example highlights the important fact that, at present, THV selection remains a multifactorial decision based on a number of clinical and imaging factors and that imaging tools such as CT or echocardiography can merely provide guidance for THV selection. The potential to underfill the expansion balloon at the time of valve deployment to achieve a smaller nominal area is being explored, but data remain quite limited. Given these limitations, as THV sizing more formally integrates 3D measurements, particularly from CT, a more meticulous and granular approach to THV sizing will almost certainly ensue. As a result, it seems likely that a larger number of THV sizes will be introduced, allowing for a more accurate and patient-specific selection of valve size.

Landing-Zone Calcification as a Predictive Factor for Paravalvular Regurgitation

In addition to annulus and root measurements, pre-TAVR CT data may provide information about anatomic details predisposing to paravalvular regurgitation and adverse post-TAVR outcome. Of interest to ongoing research is the extent of aortic valve calcifications, which has been recently investigated for both balloon-expandable (53,54) and self-expandable (55,56) TAVR devices, as severe calcification may impair complete apposition of the sealing skirt to the native commissures, requiring subsequent THV postdilation to mitigate paravalvular regurgitation.

Valvular calcifications can be assessed either visually and categorized as, for example, symmetric or asymmetric (Fig 6), or they may be quantified analogously to coronary calcium scoring. Calcium quantification is traditionally performed with noncontrast medium–enhanced CT data sets (57). However, a recent study reported on the use of contrast medium–enhanced CT data for quantification by increasing the threshold for calcium detection from the traditional 130 HU to 450 HU (55). The use of contrast-enhanced data sets may improve proper attribution of calcifications to the different leaflets.

A recent retrospective analysis of 110 patients who underwent self-expandable TAVR identified dense leaflet calcifications with an Agatston score of greater than 3000 at nonenhanced CT and a mass greater than 800 mg/mm^2 at contrast-enhanced CT as risk markers for immediate postdeployment paravalvular regurgitation and need for postdilation (odds ratio, 29.6; 95% confidence interval: 3.6, 242.9) (55). Similar findings were recently reported from a retrospective study of 353 patients who had undergone balloon-expandable TAVR (54). Patients with mild postdeployment paravalvular regurgitation were found to have a significantly higher valvular calcium burden than did patients without relevant paravalvular regurgitation, with device landing-zone calcification and asymmetric distribution as predictive factors of postdeployment paravalvular regurgitation (54). Distribution of calcification can be studied in more detail with allocation to the different structures of the valvular apparatus, that is, leaflet edges, commissures, and attachment sites of the cusps (53). In a study of 79 patients, calcification of commissures and of attachments sites was stronger predictor of paravalvular regurgitation than calcification of the leaflet edges (53).

To date, the investigation of valvular calcium burden has been restricted to retrospective, single-center studies, with differing methods for calcium assessment and for gauging paravalvular regurgitation. Overall, however, there is growing evidence of the important role of calcification in the development of paravalvular regurgitation and for predicting the need for postdilation, although it may be too early for general recommendations on patient and THV selection for TAVR. In case of severe calcification extending into the left ventricular outflow tract, higher THV implantation with balloon-expandable TAVR has been reported to reduce the likelihood of paravalvular regurgitation (54).

CT Evaluation of the Aortic Root beyond the Annulus

In addition to the annulus, complete anatomic characterization of the aortic root is needed for TAVR planning. Additional data points include, but are not limited to, the distance of the coronary ostia to the annulus, leaflet length, and width of the aortic sinus and the sinotubular junction as well as of the ascending aorta. These measurements are important to define the geometry of the aortic root and to predict the risk of potentially catastrophic complications, such as coronary occlusion and root rupture (15).

Figure 7

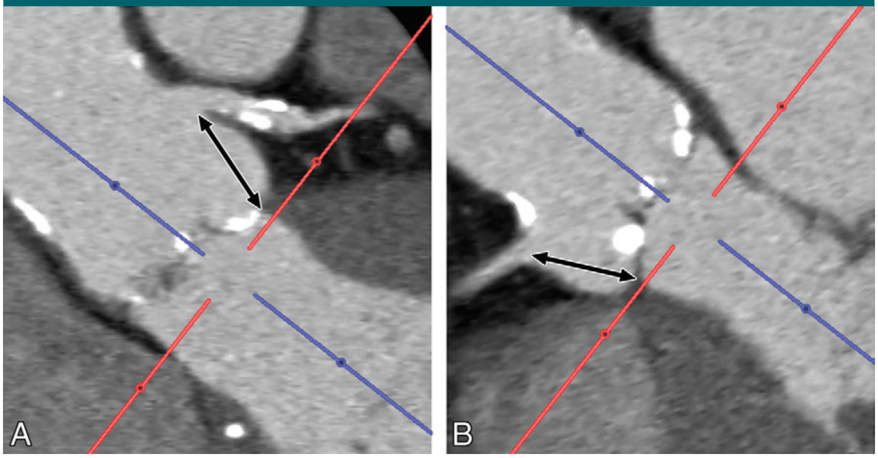

Figure 7: Contrast-enhanced retrospectively ECG-gated data set in a TAVR candidate with severe aortic stenosis displayed as double-oblique maximum intensity projections along the aortic root axis show assessment of the distance of coronary ostia from the simultaneously encompassed hinge point (arrow). *A,* Left main coronary artery with unusually high orifice at the level of the sinotubular junction. *B,* Right coronary artery.

In contrast to open valve replacement, where the native valve leaflets are resected and the annulus is decalcified, in TAVR, the native leaflets and calcifications are simply displaced and at times crushed by the THV. This harbors the risk of coronary occlusion, in particular if the coronary arteries originate low within the sinus of Valsalva, which is further augmented by small sinus and long leaflets with bulky calcifications. The distance from the aortic annulus plane to the coronary ostia can easily be assessed at CT with use of multiplanar reformations (Fig 7). In a study of 100 patients with aortic stenosis undergoing CT, the average distance of the left and right coronary ostia was 15.5 mm ± 2.9 and 17.3 mm ± 3.6, respectively (58). However, the reported average distances vary and may depend on the measurement technique (eg, oblique from hinge point to coronary ostium vs parallel to the aortic root axis) (26,58). Currently, there are no definite exclusion criteria based on the risk of coronary obstruction for both THVs discussed in this article, but an 11–14-mm distance cutoff range between the coronary ostia and the leaflet insertion has been proposed (15). In addition to the distance to the coronary ostia, other potential causes of coronary occlusion should be evaluated, including the length of the aortic valve cusps and the extent of calcification. Concern is much greater in the setting of heavily and diffusely calcified cusps than in the absence of calcification or when the calcification is isolated to the commissural insertion. We also assess the length of the left coronary cusp and its relationship to the height of the left main coronary ostium.

In contrast to the Edwards THV, the CoreValve THV is longer and extends beyond the sinotubular junction into the ascending aorta. The manufacturer's specifications require a minimum sinus of Valsalva width of 27, 29, and 29 mm for the 26-, 29-, and 31-mm, respectively, THVs and a minimum sinus of Valsalva height of 15 mm. The maximum diameter of the proximal ascending aorta should not exceed 40, 43, and 43 mm for the three THV sizes. These dimensions can easily be extracted from CT data sets.

CT-based Prediction of Angiographic Projection Angles for TAVR

In addition to annular sizing, CT can provide information about the aortic root orientation in relation to the body axis (15). For the actual valve implantation with TAVR, the interventionist requires a fluoroscopy projection oriented orthogonal to the native valve plane to ensure a coaxial deployment along the centerline of the aorta. The desired angulation can be achieved by means of multiple aortograms with stepwise optimization of the fluoroscopy unit. However, repeat aortograms result in longer procedural time, higher radiation doses and, most importantly, higher contrast medium volume. Further, if accurate orientation is not achieved, there is a risk of inappropriate positioning of the device and increased likelihood of procedural complications such as stent embolization (15,59).

The aortic valve is most commonly oriented in a cranial and anterior position with a slight degree of angulation to the right. On this basis, the interventionist typically uses a slight caudal angulation when in a right anterior oblique (RAO) projection and cranial angulation when in a left anterior oblique (LAO) projection. There are, however, significant variations in patient anatomy. The individual's aortic root orientation can be easily extracted from CT data sets to predict an appropriate angle of implantation and to reduce the need for repeat aortograms, thereby reducing procedure time, contrast medium volume, and radiation exposure (38,59). As with any disc-shaped object in a 3D space, there are numerous orthogonal projections of the native valve plane that follow a certain line of perpendicularity: Any point in the RAO to LAO spectrum can be utilized as long as the correct degree of caudal or cranial angulations is matched (60) (Fig 8, Movie 1 [online]). Given the physical constraints of a catheterization laboratory, working angles have to be realistic for use in the hybrid operating room. Common projections are *(a)* craniocaudal without RAO or LAO angulation, *(b)* straight RAO to LAO as needed without cranial or caudal angulation, and *(c)* LAO 30° with cranial or caudal angulation as needed, as suggested by Gurvitch et al (60).

Figure 8

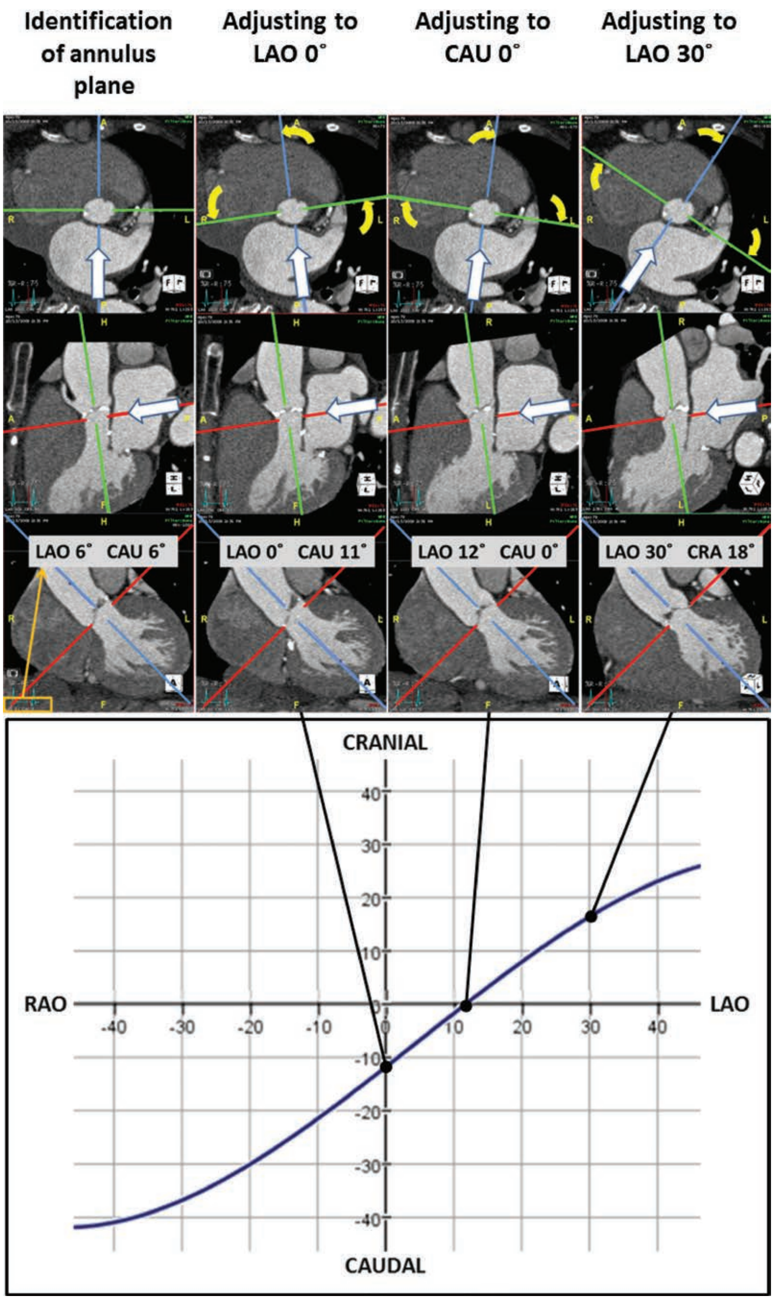

Figure 8: Prediction of orthogonal projection angles for TAVR by using multiplanar reformations. After identifying the annulus plane at the level of the basal attachments of the aortic cusps in the transverse double-oblique view (upper row), the coronal oblique view (lower row) is adjusted to achieve either a desired left anterior oblique *(LAO)* angle or a desired cranial *(CRA)*/caudal *(CAU)* angle by adjusting the cross-bars in the transverse double-oblique view (yellow arrows). Corresponding orientation angles of the resulting coronal oblique view are displayed by the postprocessing software. Orthogonal projection angles follow a line of perpendicularity, indicating the caudal or cranial angulation needed in the spectrum of right anterior oblique to LAO projections. White arrows = hypothetic direction and orientation of x-rays for fluoroscopy.

Appropriate projections are derived from CT angiographic data sets either manually by using the multiplanar reformation function of modern workflow platforms, provided that angulations are reported by the software (Fig 8), or by specifically designed applications. Recently, a number of intraprocedural technological solutions employing rotational C-arm angiographic CT (DynaCT, Siemens Healthcare Sector, Erlangen, Germany; Paieon Medical, Rosh Ha'ayin, Israel) have been introduced for use in TAVR. While these tools offer similar capacity to predict coaxial angles of deployment, these are done at the time of the procedure, unlike CT, which can provide similar information prior to the procedure. Recently, good correlation between preprocedural CT angle prediction and dynamic rotational angiography has been documented (61). An important limitation of preprocedural angle prediction with CT is patient positioning. The angles predicted from CT are only transferable to the hybrid operating suite assuming the same positioning of the patient at the time of CT and TAVR. Awareness of this important limitation is essential to optimize results and to most effectively integrate CT data into procedural planning and performance.

Iliofemoral Access: Current Data and Recommendations

The iliofemoral axis is the major route of delivery for the most commonly used THVs. Since the advent of TAVR, there have been ongoing refinements resulting in progressive reduction in the profile of the delivery systems. Current delivery profiles, as well as manufacture recommendations for minimal vessel diameters, are listed in Table 1. Single-plane angiography, which may be performed at the time of coronary artery assessment, was considered a minimum requirement for evaluation of the iliofemoral access route when TAVR first became available (12). This approach may provide adequate assessment of luminal size but only a very limited evaluation of the presence of atherosclerosis, as well as the degree of vessel tortuosity, particularly if limited to an anterior/posterior projection. Importantly, vascular complications have emerged as the major cause of mortality and morbidity when pursuing the percutaneous transfemoral approach (10,62–64). For instance, the former large 22- to 24-F sheaths required for the SAPIEN THV were associated with vascular complication rates of 22.9% in the largest European registry (62) and of 30.7% in the North American PARTNER 1B trial (10). The smaller 18-F sheaths required for the third-generation CoreValve delivery system have decreased vascular complication rates to 1.9%–13% (63,65). Of note, the reported incidence of vascular complications strongly depends on the definitions. Vascular access complications have now been formally defined by the Valve Academic Research Consortium (66) to allow for meaningful comparisons of trial end points. They provide definitions for minor and major vascular complications.

Risk factors for vascular complications of and potential contraindications to transfemoral TAVR are external sheath diameters exceeding the minimal artery diameter (depending on the device, Table 1) (6,15,67), moderate or severe calcification, peripheral vascular disease, and potentially substantial vessel tortuosity (68). CT provides thin-section isotropic volume data of the iliofemoral arteries and can easily identify the presence of all these risk factors, allowing for a more definitive assessment of the access route (Fig 9, Movie 2 [online]). Prior to introduction of TAVR, CT was already routinely used for endovascular aortic aneurysm repair, optimizing procedural outcome and making prior conventional angiography dispensable (69). Studies evaluating the use of CT for assessment of the iliofemoral vasculature prior to TAVR demonstrate that a substantial proportion of patients undergoing evaluation for potential transfemoral TAVR had unsuitable iliofemoral vasculature (32,67). One-third of patients with severe aortic stenosis had unfavorable iliofemoral arteries for a 24-F delivery system; in addition, nearly 80% of the patients evaluated had minimal luminal diameters of less than 8 mm (67).

Figure 9

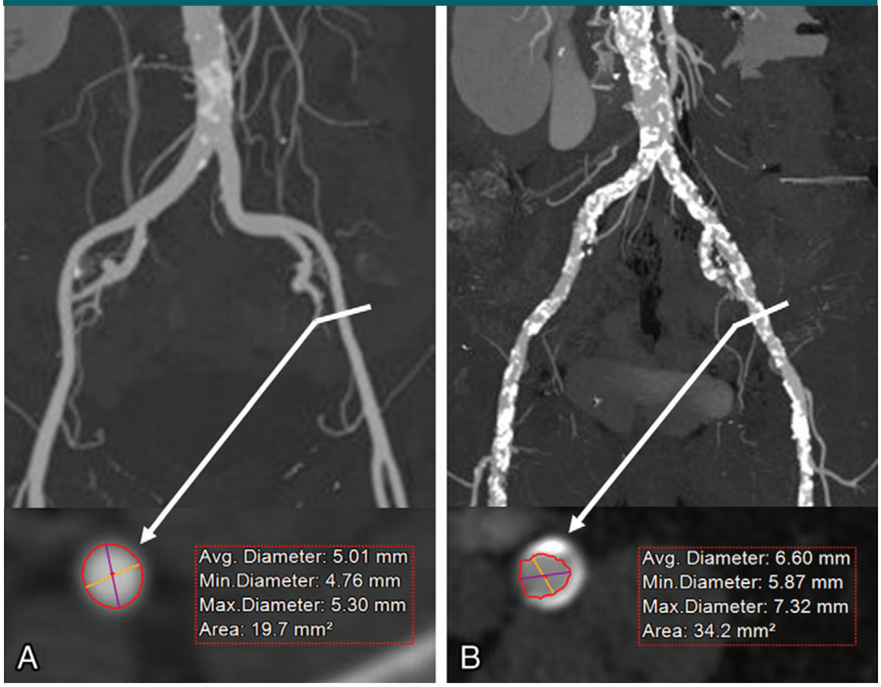

Figure 9: Contrast-enhanced CT angiographic data sets of the iliofemoral access route displayed as coronal maximum intensity projections and sections orthogonal to the centerline in curved maximum intensity projections in, *A,* an 82-year-old woman with only minor calcification of the iliac arteries but small vessel anatomy and, *B,* an 84-year-old woman with extensive, horseshoe calcifications of the iliac arteries and borderline vessel calibers, to assess suitability for transfemoral TAVR deployment. *Avg.* = average, *Min.* = minimum, *Max.* = maximum. White arrow = level of measurements.

Calcifications are of particular significance, if they are arranged in a circumferential or horseshoe-like pattern (Fig 9), especially when borderline vessel diameters are present. Such calcifications will limit arterial expandability to accommodate large-profile delivery sheaths, potentially increasing the risk of dissection or perforation. Circumferential calcifications may not be appreciated at single-plane angiography, underlining the added value of CT (15,70). The minimal lumen diameter should exceed the diameter of the delivery system; however, in our experience minimal luminal diameters 1–2 mm smaller than the external sheath diameter do not necessarily preclude transfemoral TAVR if restricted to short segments and in the absence of severe calcification. The routine integration of CT, in combination with further reductions in delivery system calibers, provides an opportunity to decrease the rate of vascular complications. This improvement in outcomes has recently been realized in some centers, who report a decrease of major vascular complications from 8% to 1% and of minor vascular complications from 24% to 8% between 2009 and 2010 (68). Importantly, CT was a strong predictor of vascular complications when the minimal artery diameter was less than the external sheath diameter and in the setting of moderate to severe vascular calcification. Although often discussed in the literature, the risk arising from vessel tortuosity is uncertain, in part, due to a lack of a simple measure. In our experience, tortuosity in isolation is not a contraindication to TAVR and ilio-

Table 3

Summary of Essential Imaging Findings and Suggested Items for Inclusion in the CT Report

Item	Finding
Aortic valve	
Valve anatomy	Tricuspid, bicuspid, functionally bicuspid
Degree of calcification	Mild, moderate, severe
Distribution of calcifications	Symmetric, asymmetric, extent of calcifications into LVOT
Aortic root dimensions	Area or perimeter derived annulus diameter, short- and long-axis dimensions, distance of right and left coronary ostia to the annulus level and leaflet length, diameter of the aortic sinus, diameter of the sinotubular junction
Aortic root orientation (orthogonal projection angles)	Required RAO/LAO angulation for 0° cranial/caudal angulation, required cranial/caudal angulation for 0° RAO/LAO angulation, required cranial angulation for 30° LAO angulation
Coronary anatomy	Anatomy, anomalies
Ascending aorta and arch	
Dimensions	Maximal diameter of the ascending aorta
Disease	Calcifications and atheromatous plaque
Descending and abdominal aorta	Course, tortuosity, and presence of aneurysms
Iliofemoral access route	
Tortuosity	…
Calcifications	None, mild, moderate, severe; presence of horseshoe or circumferential calcifications; particular emphasis on calcification of common femoral artery*
Diameter	Diameter of common iliac, external iliac, and common femoral artery
Subclavian artery	
Diameter	…
Disease	Stenosis

Note.—LAO = left anterior oblique, LVOT = left ventricular outflow tract, RAO = right anterior oblique.

* Of particular importance when percutaneous approach is intended with usage of percutaneous suture system.

Figure 10

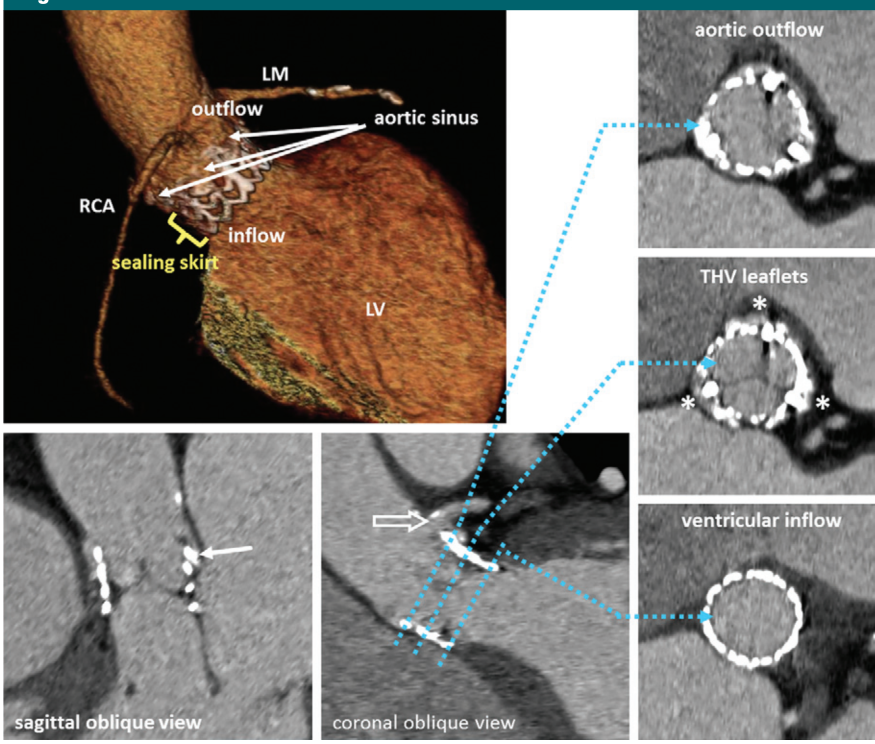

Figure 10: Postdeployment contrast-enhanced retrospectively ECG-gated CT study after TAVR with balloon-expandable SAPIEN THV with optimal position. Volume-rendered reconstruction and multiplanar reformations show THV position in relation to the aortic sinus and left main (*LM,* open arrow) and right coronary arteries *(RCA).* Native valvular calcifications (solid arrows) are displaced into the aortic sinus (*), while the coronary orifices are preserved. The THV is circularly unfolded at all levels and shows complete apposition with its entire circumference at its inflow level to the upper left ventricular outflow tract.

Figure 11

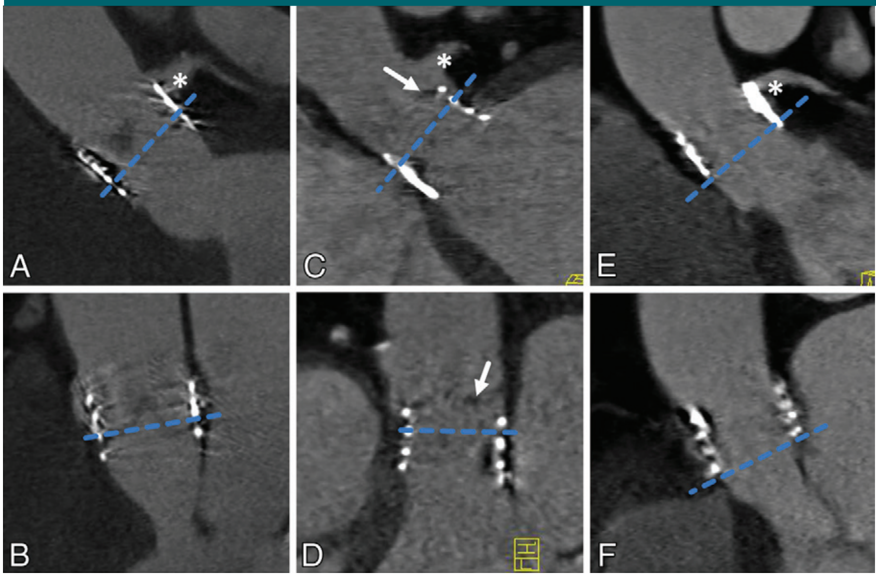

Figure 11: Postdeployment contrast-enhanced retrospectively ECG-gated CT studies after TAVR with balloon-expandable SAPIEN THV in three patients with, *A, B,* optimal, *C, D,* low, and, *E, F,* too high inflow position relative to the native annulus plane. Upper row are coronal oblique reconstructions; lower row are sagittal oblique views, similar to parasternal long-axis views at echocardiography. Dashed blue lines = native annulus plane. Native valve leaflets overly THV outflow with too low positioning (arrow). Even with optimal positioning, THV struts may partially overly the coronary ostia (*). With too high positioning, coronary stent struts overly the left coronary ostium; however, with the THV seal confined to the lower two-thirds of the prosthesis, this does not imply coronary ostium occlusion.

Figure 12

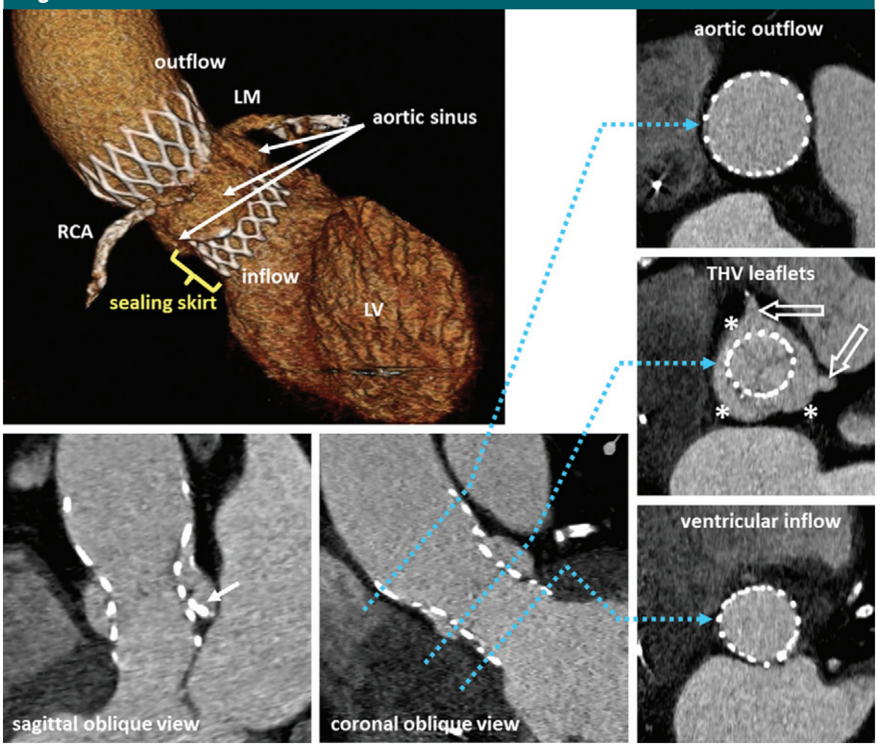

Figure 12: Postdeployment contrast-enhanced retrospectively ECG-gated CT study after TAVR with self-expandable CoreValve with optimal position. Volume-rendered reconstruction and multiplanar reformations depict THV position in relation to the aortic sinus and left main *(LM)* and right coronary arteries *(RCA)*. Native valvular calcifications are displaced into the aortic sinus (solid arrows), while coronary orifices (open arrows) and sinus are preserved due to THV's constrained zone in its midportion. The THV is circularly unfolded at all levels and shows complete apposition with its entire circumference at its inflow level to the upper left ventricular outflow tract.

femoral tortuosity 45° or greater does not appear to predict vascular complications (68). However, in the setting of borderline vessel caliber and significant calcification burden, tortuosity may introduce an additional element of risk by adding further friction onto the delivery system, which may impact the advancement of and control over the catheter-based deployment system.

CT for TAVR Access Evaluation

CT for TAVR access evaluation usually includes 3D volume-rendered image display, curved multiplanar reformats, and maximum intensity projections. Multiple measurements are taken along the entire course of the iliofemoral system bilaterally, with the minimum luminal measurement recorded for each side and included in the report (Table 3, Fig 9). A description of the overall plaque burden and presence of iliofemoral calcification should also be provided. Identification of the specific location of areas with reduced luminal size is important. In some cases, access can be achieved proximal to the site with a cut-down approach. Particular attention is paid to any regions of circumferential or horseshoe calcification. Importantly, the minimal luminal diameter should be provided along the en-

Figure 13

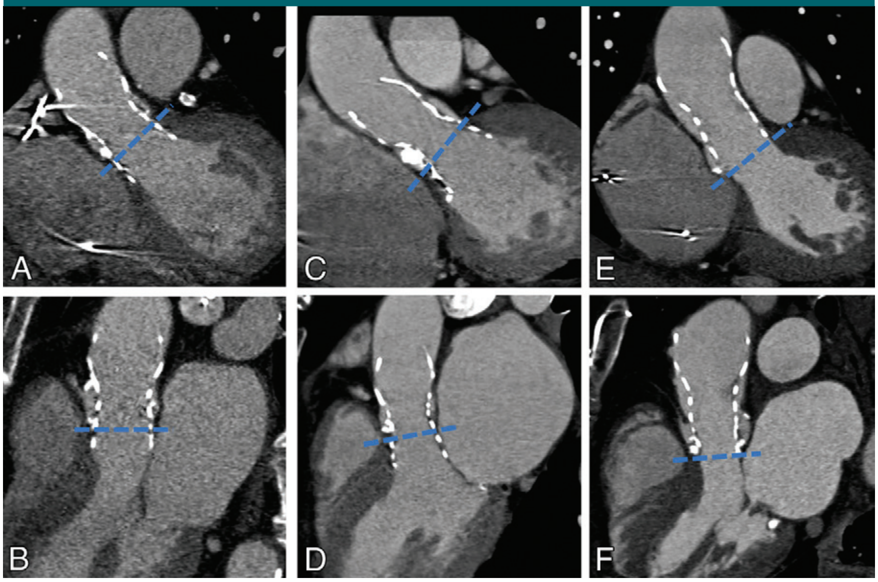

Figure 13: Postdeployment contrast-enhanced retrospectively ECG-gated CT studies after TAVR with the self-expandable CoreValve THV in three patients with *A, B,* optimal, *C, D,* low, and, *E, F,* too high inflow position relative to the native annulus plane. Dashed blue lines = level of native aortic annulus. Upper row are coronal oblique reconstructions; lower row are sagittal oblique views, similar to parasternal long-axis views at echocardiography.

Figure 14

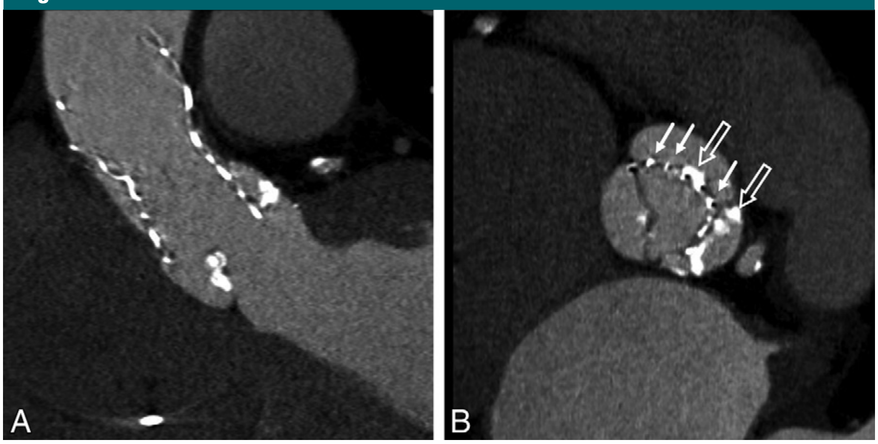

Figure 14: Postdeployment contrast-enhanced retrospectively ECG-gated CT study reveals migration of a self-expandable THV from the annulus plane occurring with too high deployment (systolic image reconstructions). *A,* Coronal oblique view shows the THV inflow is partially dislodged from the aortic valve. *B,* Transverse double-oblique view at the level of the inflow shows that only the right and left coronary cusps are still in contact with the THV struts (solid arrows), while the noncoronary cusp is not encompassed by THV (open arrows mark native valve calcifications).

tire course of both the right and left iliofemoral system down to the femoral head. If applicable, the report may include a recommendation on the favorable side.

CT is also a helpful adjunct for the evaluation of other access routes. CT can depict atheroma or bulky calcifications in the aortic arch (22), which might incur the risk of stroke when dislodged by mechanic manipulation during an intervention (18). In the setting of unfavorable iliofemoral anatomy, a subclavian or trans-apical approach may be selected. CT can provide similar anatomic detail for the subclavian system, as well as preprocedural localization of the left ventricular apex, to assist with the transapical puncture.

Concomitant Cardiac Disease

The extent and degree of left ventricular hypertrophy, particularly involving the basal septum, and the angle between the aorta and the left ventricle are important in planning the TAVR procedure. A septal bulge extending into the left ventricular outflow tract can provide a challenge to the operator at the time of valve deployment and can conceivably result in malpositioning, particularly at the termination of the pacing run. Left ventricular dysfunction can also influence the strategy for performing TAVR. As an example, it is generally accepted that in patients with severely depressed left ventricular function the number of pacing runs should be minimized to decrease the likelihood of hemodynamic compromise. There also needs to be an awareness of the presence of pre-existing aortic regurgitation, as balloon dilation may worsen the severity of aortic insufficiency and cause hemodynamic compromise (71). As with most aspects in TAVR, preparation is of utmost importance as rapid deployment of the valve is necessary in the setting of aortic regurgitation.

Post-TAVR Imaging: Expected and Unexpected Findings

Although technically limited by its two-dimensional nature, prosthesis position can be assessed on the routinely obtained postdeployment angiogram. Furthermore, intraoperative transesophageal echocardiography aids in the demonstration of appropriate prosthesis function and positioning and for evaluating paravalvular regurgitation. To date, there is no formal recommendation on performing routine follow-up CT angiographic studies in TAVR recipients. The

Figure 15

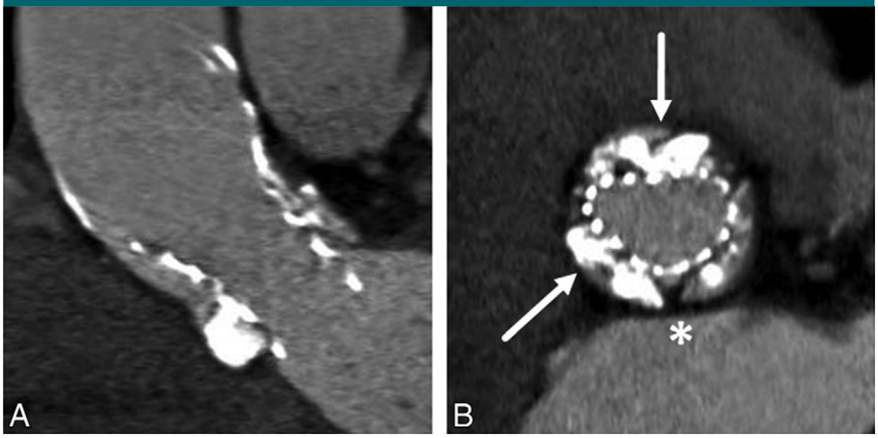

Figure 15: Postdeployment contrast-enhanced retrospectively ECG-gated CT study after self-expandable TAVR in a patient with severe native valve calcifications. Postdeployment transverse double-oblique CT views reveal, *A,* too high positioning of the THV inflow with, *B,* incomplete expansion of the inflow due to bulky calcifications (arrows), as well as incomplete apposition of the native commissure between the noncoronary and left coronary cusp (*), giving rise to paravalvular regurgitation.

Figure 16

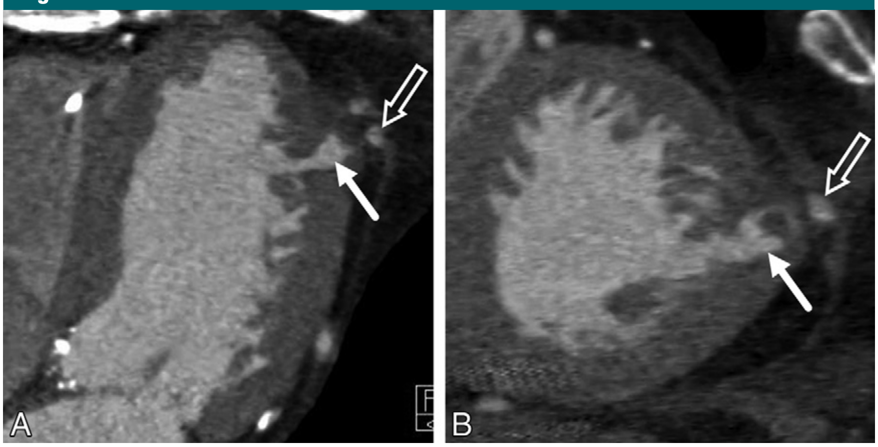

Figure 16: Postdeployment contrast-enhanced retrospectively ECG-gated, *A,* long-axis and, *B,* short-axis CT views reveal contrast medium–filled outpouching of the latero-apical wall of the left ventricle, diagnostic of a suture aneurysm (solid arrow). Cannulation of the true apex was not performed due to relative median position. Focal pericardial hyperattenuating structure resembles suture material (open arrow).

risk of repeat contrast media exposure has to be weighed against the clinical benefit and the likelihood of actual consequences, which may be limited as the high perioperative mortality risk will often preclude corrective surgery for complications in patients treated with TAVR. At our institutions, we perform follow-up CT angiography in case of equivocal findings with other imaging modalities or in patients who develop new-onset symptoms after their procedure.

However, postinterventional CT, if performed, provides direct 3D feedback to the interventionist on prosthesis positioning and may reveal underlying causes for paravalvular leaks. The typical appearance of the Edwards SAPIEN THV on postdeployment CT scans is illustrated in Figure 10. With balloon-expandable TAVR, postdeployment CT will show a circularly unfolded THV in the majority of patients (27,39,45), with native leaflet calcifications displaced toward the native sinus. An eccentric deployment (eccentricity index > 0.1) may be observed in the setting of heavy (39) and asymmetric calcifications. With ideal deployment, the ventricular inflow is located below the native annulus plane, with the outflow ending extending beyond the tips of the native leaflets (Fig 10). If the point of deployment is too high, this results in an inflow position above the basal insertion of the native leaflets. The THV is deployed too low when the outflow portion of the sealing cuff (lower two-thirds) is positioned below the most basal attachment points (Fig 11). Importantly, THV struts may overlay the coronary ostia, in particular in patients with low sinus heights. This does not imply ostia occlusion, as the upper third of the THV is not covered by a sealing cuff (Figs 1, 10).

Postdeployment CT findings are remarkably different with the CoreValve THV. The typical appearance of the CoreValve THV on postdeployment CT angiogram is illustrated in Figure 12. Due to the self-expandable nature of the device, its postdeployment geometry is naturally more adaptive to underlying anatomy, extent, and degree of native leaflet calcifications, while native annulus geometry is preserved. If correctly positioned (tips of ventricular struts 5–10 mm below the annulus plane, Fig 12), the ventricular inflow is most often incompletely expanded, while the constrained part of the THV with its supra-annular valve is more uniformly expanded (72). If deployed too high (Fig 13), the ventricular inflow may eventually migrate out of the valvular apparatus (Fig 14) and the inflow may be partially covered by the native leaflets.

From our own experience, postdeployment CT may provide explanations for postprocedural paravalvular regurgitation, such as incomplete apposition of the native commissures (Fig 15). However, optimal THV positioning and expansion at CT does not rule out paravalvular regurgitation. Further complications confined to the aortic

Figure 17

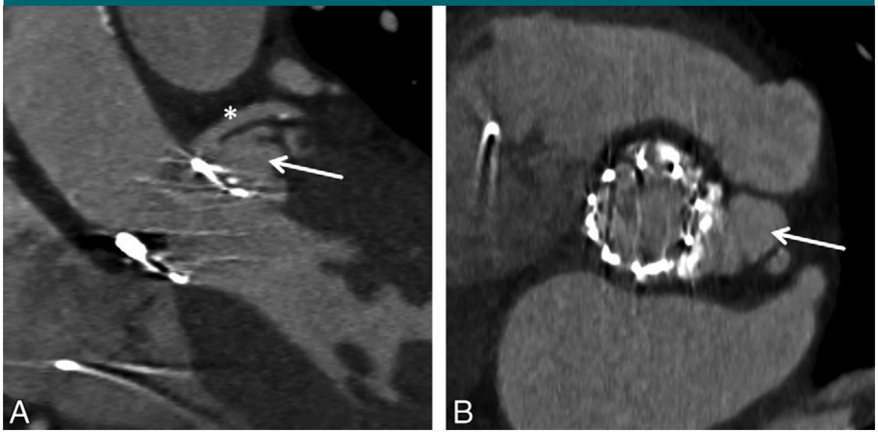

Figure 17: *A,* Coronal oblique and, *B,* transverse double-oblique images of contrast-enhanced retrospectively ECG-gated CT study in an asymptomatic 84-year-old woman who underwent routine post-TAVR CT on postoperative day 7 reveal correct THV positioning. However, a contrast medium–filled aneurysm (arrow) is discernible adjacent to the aortic root at the position of the native left coronary cusp, originating from the left ventricular outflow tract, establishing the diagnosis of contained aortic root rupture. Close relation to the left main coronary artery (*) can be appreciated.

root and heart are coronary obstruction, cardiac tamponade, aortic root rupture, aortic dissection, suture aneurysms (Fig 16) with the transapical approach (73), and contained rupture (50) with formation of pseudoaneurysms (Fig 17).

CT Assessment of Structural and Functional THV Integrity

Similar to endovascular aortic repair (74), long-term durability of the THV is of major concern. Given the different components of THVs, the following aspects are of interest: structural integrity of the stent frame, absence of valve recoil and migration, and leaflet integrity and durability. CT is capable of evaluating the stent frame and position and thus may provide evidence of long-term durability. Furthermore, CT may depict leaflet thickening or calcifications. Data on THV longevity are currently limited. In a study of 21 patients at a minimum of 3 years after implantation of a balloon-expandable THV, CT did not show any evidence of stent fracture or leaflet degeneration, while it demonstrated preserved circularity of the stent frame (75). Recently, these findings were confirmed in a larger study of 50 patients at more than 1 year after balloon-expandable TAVR. Of note, as documented with CT, circularity was present in 96% of patients, maintaining full expansion without stent fracture at an average of 2.5 years after TAVR (76). In a subset of eight patients with immediate postimplant CT scans, serial comparison did not reveal evidence of stent migration as assessed by the distance from the top of the stent to the origin of the left coronary ostium (75). This single-center evidence has to be validated in a larger scale study for the balloon-expandable THVs. There is even greater paucity of long-term follow-up CT data for the CoreValve THV. So far, long-term structural integrity of the CoreValve THV has only been assessed at plain fluoroscopy (77).

Conclusion

TAVR has seen substantial advancements over recent years, with rapidly growing data supporting its use and demonstrating satisfactory midterm outcomes. While echocardiography remains an integral component of TAVR imaging, CT with its 3D imaging capabilities provides robust assessment of annular and aortic root morphology and dimensions, which provides critical incremental information. At the same time, this modality uniquely allows for simultaneous assessment of iliofemoral access and angiographic angle prediction. With ongoing device development and the integration of advanced imaging methods, such as CT, there will almost certainly be continued improvement in the safety profile and a potential for further broadening of the indication of TAVR in the management of symptomatic aortic stenosis.

Disclosures of Conflicts of Interest: P.B. No relevant conflicts of interest to disclose. **U.J.S.** Financial activities related to the present article: none to disclose. Financial activities not related to the present article: author received consultancy fees from Bayer, Bracco, GE, Medrad, Siemens; institution received a grant from Bayer, Bracco, GE, Medrad, Siemens; author received payment for lectures including service on speakers bureaus; institution received payment from GE for development of educational presentations. Other relationships: none to disclose. **J.A.L.** Financial activities related to the present article: author is a consultant for GE, provided core lab services to Edwards Lifesciences. Financial activities not related to the present article: author received board membership fees, consultancy fees, payment for lectures including service on speakers bureaus, and payment for development of educational presentations from GE and Edwards Lifesciences. Other relationships: none to disclose.

References

1. Iung B, Baron G, Butchart EG, et al. A prospective survey of patients with valvular heart disease in Europe: The Euro Heart Survey on Valvular Heart Disease. Eur Heart J 2003;24(13):1231–1243.
2. Nkomo VT, Gardin JM, Skelton TN, Gottdiener JS, Scott CG, Enriquez-Sarano M. Burden of valvular heart diseases: a population-based study. Lancet 2006; 368(9540):1005–1011.
3. American College of Cardiology/American Heart Association Task Force on Practice GuidelinesSociety of Cardiovascular AnesthesiologistsSociety for Cardiovascular Angiography and Interventions et al. ACC/AHA 2006 guidelines for the management of patients with valvular heart disease: a report of the American College of Cardiology/American Heart Association Task Force on Practice Guidelines (writing committee to revise the 1998 guidelines for the management of patients with valvular heart disease) developed in collaboration with the Society of Cardiovascular Anesthesiologists en-

dorsed by the Society for Cardiovascular Angiography and Interventions and the Society of Thoracic Surgeons. Circulation 2006;114(5):e84–e231. [Published corrections appear in Circulation 2007;115(15): e409 and Circulation 2010;121(23):e443.]

4. Vahanian A, Baumgartner H, Bax J, et al. Guidelines on the management of valvular heart disease: the Task Force on the Management of Valvular Heart Disease of the European Society of Cardiology. Eur Heart J 2007;28(2):230–268.

5. Iung B, Cachier A, Baron G, et al. Decision-making in elderly patients with severe aortic stenosis: why are so many denied surgery? Eur Heart J 2005;26(24):2714–2720.

6. Webb JG, Chandavimol M, Thompson CR, et al. Percutaneous aortic valve implantation retrograde from the femoral artery. Circulation 2006;113(6):842–850.

7. Lichtenstein SV, Cheung A, Ye J, et al. Transapical transcatheter aortic valve implantation in humans: initial clinical experience. Circulation 2006;114(6):591–596.

8. Grube E, Laborde JC, Gerckens U, et al. Percutaneous implantation of the CoreValve self-expanding valve prosthesis in high-risk patients with aortic valve disease: the Siegburg first-in-man study. Circulation 2006; 114(15):1616–1624.

9. Holmes DR Jr, Mack MJ, Kaul S, et al. 2012 ACCF/AATS/SCAI/STS expert consensus document on transcatheter aortic valve replacement. J Am Coll Cardiol 2012;59(13): 1200–1254.

10. Leon MB, Smith CR, Mack M, et al. Transcatheter aortic-valve implantation for aortic stenosis in patients who cannot undergo surgery. N Engl J Med 2010;363(17):1597–1607.

11. Smith CR, Leon MB, Mack MJ, et al. Transcatheter versus surgical aortic-valve replacement in high-risk patients. N Engl J Med 2011;364(23):2187–2198.

12. Vahanian A, Alfieri O, Al-Attar N, et al. Transcatheter valve implantation for patients with aortic stenosis: a position statement from the European Association of Cardio-Thoracic Surgery (EACTS) and the European Society of Cardiology (ESC), in collaboration with the European Association of Percutaneous Cardiovascular Interventions (EAPCI). Eur Heart J 2008;29(11): 1463–1470.

13. Binder RK, Webb JG, Willson AB, et al. The impact of integration of a multidetector computed tomography annulus area sizing algorithm on outcomes of transcatheter aortic valve replacement: a prospective, multicenter, controlled trial. J Am Coll Cardiol 2013;62(5):431–438.

14. Webb JG, Altwegg L, Masson JB, Al Bugami S, Al Ali A, Boone RA. A new transcatheter aortic valve and percutaneous valve delivery system. J Am Coll Cardiol 2009;53(20): 1855–1858.

15. Masson JB, Kovac J, Schuler G, et al. Transcatheter aortic valve implantation: review of the nature, management, and avoidance of procedural complications. JACC Cardiovasc Interv 2009;2(9):811–820.

16. Kodali SK, Williams MR, Smith CR, et al. Two-year outcomes after transcatheter or surgical aortic-valve replacement. N Engl J Med 2012;366(18):1686–1695.

17. Thomas M, Schymik G, Walther T, et al. One-year outcomes of cohort 1 in the Edwards SAPIEN Aortic Bioprosthesis European Outcome (SOURCE) registry: the European registry of transcatheter aortic valve implantation using the Edwards SAPIEN valve. Circulation 2011;124(4):425–433.

18. Safety and efficacy study of the Medtronic CoreValve System in the treatment of symptomatic severe aortic stenosis in high risk and very high risk subjects who need aortic valve replacement. http://clinicaltrials.gov/ct2/show/NCT01240902. Accessed February 15, 2012.

19. Ussia GP, Barbanti M, Petronio AS, et al. Transcatheter aortic valve implantation: 3-year outcomes of self-expanding CoreValve prosthesis. Eur Heart J 2012;33(8): 969–976.

20. Zoghbi WA, Chambers JB, Dumesnil JG, et al. Recommendations for evaluation of prosthetic valves with echocardiography and doppler ultrasound: a report From the American Society of Echocardiography's Guidelines and Standards Committee and the Task Force on Prosthetic Valves, developed in conjunction with the American College of Cardiology Cardiovascular Imaging Committee, Cardiac Imaging Committee of the American Heart Association, the European Association of Echocardiography, a registered branch of the European Society of Cardiology, the Japanese Society of Echocardiography and the Canadian Society of Echocardiography, endorsed by the American College of Cardiology Foundation, American Heart Association, European Association of Echocardiography, a registered branch of the European Society of Cardiology, the Japanese Society of Echocardiography, and Canadian Society of Echocardiography. J Am Soc Echocardiogr 2009;22(9): 975–1014; quiz 1082–1084.

21. Abdel-Wahab M, Zahn R, Horack M, et al. Aortic regurgitation after transcatheter aortic valve implantation: incidence and early outcome—results from the German transcatheter aortic valve interventions registry. Heart 2011;97(11):899–906.

22. Athappan G, Patvardhan E, Tuzcu EM, et al. Incidence, predictors, and outcomes of aortic regurgitation after transcatheter aortic valve replacement: meta-analysis and systematic review of literature. J Am Coll Cardiol 2013;61(15):1585–1595.

23. Anderson RH. Clinical anatomy of the aortic root. Heart 2000;84(6):670–673.

24. Piazza N, de Jaegere P, Schultz C, Becker AE, Serruys PW, Anderson RH. Anatomy of the aortic valvar complex and its implications for transcatheter implantation of the aortic valve. Circ Cardiovasc Interv 2008; 1(1):74–81.

25. Ng AC, Delgado V, van der Kley F, et al. Comparison of aortic root dimensions and geometries before and after transcatheter aortic valve implantation by 2- and 3-dimensional transesophageal echocardiography and multislice computed tomography. Circ Cardiovasc Imaging 2010;3(1):94–102.

26. Tops LF, Wood DA, Delgado V, et al. Noninvasive evaluation of the aortic root with multislice computed tomography implications for transcatheter aortic valve replacement. JACC Cardiovasc Imaging 2008;1(3): 321–330.

27. Blanke P, Siepe M, Reinöhl J, et al. Assessment of aortic annulus dimensions for Edwards SAPIEN Transapical Heart Valve implantation by computed tomography: calculating average diameter using a virtual ring method. Eur J Cardiothorac Surg 2010;38(6):750–758.

28. Hamdan A, Guetta V, Konen E, et al. Deformation dynamics and mechanical properties of the aortic annulus by 4-dimensional computed tomography: insights into the functional anatomy of the aortic valve complex and implications for transcatheter aortic valve therapy. J Am Coll Cardiol 2012;59(2):119–127.

29. Veronesi F, Corsi C, Sugeng L, et al. A study of functional anatomy of aortic-mitral valve coupling using 3D matrix transesophageal echocardiography. Circ Cardiovasc Imaging 2009;2(1):24–31.

30. Rodés-Cabau J, DeLarochellière R, Dumont E. First-in-man transcatheter aortic valve implantation of a 20-mm Edwards SAPIEN XT valve: one step forward for the treatment of patients with severe aortic stenosis and small aortic annulus. Catheter Cardiovasc Interv 2012;79(5):789–793.

31. Blanke P, Russe M, Leipsic J, et al. Conformational pulsatile changes of the aortic annulus: impact on prosthesis sizing by computed tomography for transcatheter aortic valve replacement. JACC Cardiovasc Interv 2012;5(9):984–994.

32. Blanke P, Euringer W, Baumann T, et al. Combined assessment of aortic root anatomy and aortoiliac vasculature with dual-source CT as a screening tool in patients evaluated for transcatheter aortic valve implantation. AJR Am J Roentgenol 2010; 195(4):872–881.

33. Lange R, Bleiziffer S, Piazza N, et al. Incidence and treatment of procedural cardiovascular complications associated with trans-arterial and trans-apical interventional aortic valve implantation in 412 consecutive patients. Eur J Cardiothorac Surg 2011; 40(5):1105–1113.

34. Wuest W, Anders K, Schuhbaeck A, et al. Dual source multidetector CT-angiography before transcatheter aortic valve implantation (TAVI) using a high-pitch spiral acquisition mode. Eur Radiol 2012;22(1):51–58.

35. Joshi SB, Mendoza DD, Steinberg DH, et al. Ultra-low-dose intra-arterial contrast injection for iliofemoral computed tomographic angiography. JACC Cardiovasc Imaging 2009;2(12):1404–1411.

36. Nietlispach F, Leipsic J, Al-Bugami S, Masson JB, Carere RG, Webb JG. CT of the ilio-femoral arteries using direct aortic contrast injection: proof of feasibility in patients screened towards percutaneous aortic valve replacement. Swiss Med Wkly 2009; 139(31-32):458–462.

37. Schultz CJ, Moelker A, Piazza N, et al. Three dimensional evaluation of the aortic annulus using multislice computer tomography: are manufacturer's guidelines for sizing for percutaneous aortic valve replacement helpful? Eur Heart J 2010; 31(7):849–856.

38. Gurvitch R, Webb JG, Yuan R, et al. Aortic annulus diameter determination by multidetector computed tomography: reproducibility, applicability, and implications for transcatheter aortic valve implantation. JACC Cardiovasc Interv 2011;4(11):1235–1245.

39. Delgado V, Ng AC, van de Veire NR, et al. Transcatheter aortic valve implantation: role of multi-detector row computed tomography to evaluate prosthesis positioning and deployment in relation to valve function. Eur Heart J 2010;31(9):1114–1123.

40. Messika-Zeitoun D, Serfaty JM, Brochet E, et al. Multimodal assessment of the aortic annulus diameter: implications for transcatheter aortic valve implantation. J Am Coll Cardiol 2010;55(3):186–194.

41. Tzikas A, Schultz CJ, Piazza N, et al. Assessment of the aortic annulus by multislice computed tomography, contrast aortography, and trans-thoracic echocardiography in patients referred for transcatheter aortic valve implantation. Catheter Cardiovasc Interv 2011;77(6):868–875.

42. Anderson RH, Lal M, Ho SY. Anatomy of the aortic root with particular emphasis on options for its surgical enlargement. J Heart Valve Dis 1996;5(Suppl 3):S249–S257.

43. Leipsic J, Gurvitch R, Labounty TM, et al. Multidetector computed tomography in transcatheter aortic valve implantation. JACC Cardiovasc Imaging 2011;4(4):416–429.

44. Webb JG, Altwegg L, Boone RH, et al. Transcatheter aortic valve implantation: impact on clinical and valve-related outcomes. Circulation 2009;119(23):3009–3016.

45. Willson AB, Webb JG, Labounty TM, et al. 3-dimensional aortic annular assessment by multidetector computed tomography predicts moderate or severe paravalvular regurgitation after transcatheter aortic valve replacement: a multicenter retrospective analysis. J Am Coll Cardiol 2012;59(14):1287–1294.

46. Jabbour A, Ismail TF, Moat N, et al. Multimodality imaging in transcatheter aortic valve implantation and post-procedural aortic regurgitation: comparison among cardiovascular magnetic resonance, cardiac computed tomography, and echocardiography. J Am Coll Cardiol 2011;58(21):2165–2173.

47. Jilaihawi H, Kashif M, Fontana G, et al. Cross-sectional computed tomographic assessment improves accuracy of aortic annular sizing for transcatheter aortic valve replacement and reduces the incidence of paravalvular aortic regurgitation. J Am Coll Cardiol 2012;59(14):1275–1286.

48. Hansson NC, Thuesen L, Hjortdal VE, et al. Three-dimensional multidetector computed tomography versus conventional 2-dimensional transesophageal echocardiography for annular sizing in transcatheter aortic valve replacement: influence on postprocedural paravalvular aortic regurgitation. Catheter Cardiovasc Interv 2013.

49. Jilaihawi H, Doctor N, Kashif M, et al. Aortic annular sizing for transcatheter aortic valve replacement using cross-sectional 3-dimensional transesophageal echocardiography. J Am Coll Cardiol 2013;61(9):908–916.

50. Blanke P, Reinöhl J, Schlensak C, et al. Prosthesis oversizing in balloon-expandable transcatheter aortic valve implantation is associated with contained rupture of the aortic root. Circ Cardiovasc Interv 2012;5(4):540–548.

51. Barbanti M, Yang TH, Rodès Cabau J, et al. Anatomical and procedural features associated with aortic root rupture during balloon-expandable transcatheter aortic valve replacement. Circulation 2013;128(3):244–253.

52. Piazza N, Lange R. Imaging of valvular heart disease: I can see clearly now—anatomy of the aortic valve. http://org.crsti.dliv2010.s3.amazonaws.com/pdfs/034_Ovality_of_the_aortic_valve_annulus.pdf. Published 2010. Accessed April 15, 2011.

53. Ewe SH, Ng AC, Schuijf JD, et al. Location and severity of aortic valve calcium and implications for aortic regurgitation after transcatheter aortic valve implantation. Am J Cardiol 2011;108(10):1470–1477.

54. Unbehaun A, Pasic M, Dreysse S, et al. Transapical aortic valve implantation: incidence and predictors of paravalvular leakage and transvalvular regurgitation in a series of 358 patients. J Am Coll Cardiol 2012;59(3):211–221.

55. Schultz C, Rossi A, van Mieghem N, et al. Aortic annulus dimensions and leaflet calcification from contrast MSCT predict the need for balloon post-dilatation after TAVI with the Medtronic CoreValve prosthesis. EuroIntervention 2011;7(5):564–572.

56. John D, Buellesfeld L, Yuecel S, et al. Correlation of Device landing zone calcification and acute procedural success in patients undergoing transcatheter aortic valve implantations with the self-expanding CoreValve prosthesis. JACC Cardiovasc Interv 2010;3(2):233–243.

57. Morgan-Hughes GJ, Owens PE, Roobottom CA, Marshall AJ. Three dimensional volume quantification of aortic valve calcification using multislice computed tomography. Heart 2003;89(10):1191–1194.

58. Stolzmann P, Knight J, Desbiolles L, et al. Remodelling of the aortic root in severe tricuspid aortic stenosis: implications for transcatheter aortic valve implantation. Eur Radiol 2009;19(6):1316–1323.

59. Kurra V, Kapadia SR, Tuzcu EM, et al. Preprocedural imaging of aortic root orientation and dimensions: comparison between X-ray angiographic planar imaging and 3-dimensional multidetector row computed tomography. JACC Cardiovasc Interv 2010;3(1):105–113.

60. Gurvitch R, Wood DA, Leipsic J, et al. Multislice computed tomography for prediction of optimal angiographic deployment projections during transcatheter aortic

valve implantation. JACC Cardiovasc Interv 2010;3(11):1157–1165.

61. Binder RK, Leipsic J, Wood D, et al. Prediction of optimal deployment projection for transcatheter aortic valve replacement: angiographic 3-dimensional reconstruction of the aortic root versus multidetector computed tomography. Circ Cardiovasc Interv 2012;5(2):247–252.

62. Thomas M, Schymik G, Walther T, et al. Thirty-day results of the SAPIEN aortic Bioprosthesis European Outcome (SOURCE) Registry: a European registry of transcatheter aortic valve implantation using the Edwards SAPIEN valve. Circulation 2010; 122(1):62–69.

63. Van Mieghem NM, Nuis RJ, Piazza N, et al. Vascular complications with transcatheter aortic valve implantation using the 18 Fr Medtronic CoreValve System: the Rotterdam experience. EuroIntervention 2010; 5(6):673–679.

64. Eltchaninoff H, Prat A, Gilard M, et al. Transcatheter aortic valve implantation: early results of the FRANCE (FRench Aortic National CoreValve and Edwards) registry. Eur Heart J 2011;32(2):191–197.

65. Piazza N, Grube E, Gerckens U, et al. Procedural and 30-day outcomes following transcatheter aortic valve implantation using the third generation (18 Fr) corevalve revalving system: results from the multicentre, expanded evaluation registry 1-year following CE mark approval. EuroIntervention 2008;4(2):242–249.

66. Leon MB, Piazza N, Nikolsky E, et al. Standardized endpoint definitions for Transcatheter Aortic Valve Implantation clinical trials: a consensus report from the Valve Academic Research Consortium. J Am Coll Cardiol 2011;57(3):253–269.

67. Kurra V, Schoenhagen P, Roselli EE, et al. Prevalence of significant peripheral artery disease in patients evaluated for percutaneous aortic valve insertion: preprocedural assessment with multidetector computed tomography. J Thorac Cardiovasc Surg 2009;137(5):1258–1264.

68. Toggweiler S, Gurvitch R, Leipsic J, et al. Percutaneous aortic valve replacement: vascular outcomes with a fully percutaneous procedure. J Am Coll Cardiol 2012;59(2): 113–118.

69. Wyers MC, Fillinger MF, Schermerhorn ML, et al. Endovascular repair of abdominal aortic aneurysm without preoperative arteriography. J Vasc Surg 2003;38(4):730–738.

70. Descoutures F, Himbert D, Lepage L, et al. Contemporary surgical or percutaneous management of severe aortic stenosis in the elderly. Eur Heart J 2008;29(11): 1410–1417.

71. Jilaihawi H, Makkar R, Hussaini A, Trento A, Kar S. Contemporary application of cardiovascular hemodynamics: transcatheter mitral valve interventions. Cardiol Clin 2011;29(2):201–209.

72. Schultz CJ, Weustink AC, Piazza N, et al. Geometry and degree of apposition of the CoreValve ReValving system with multislice computed tomography after implantation in patients with aortic stenosis. J Am Coll Cardiol 2009;54(10):911–918.

73. Pasic M, Buz S, Dreysse S, et al. Transapical aortic valve implantation in 194 patients: problems, complications, and solutions. Ann Thorac Surg 2010;90(5):1463–1469; discussion 1469–1470.

74. Hiratzka LF, Bakris GL, Beckman JA, et al. 2010 ACCF/AHA/AATS/ACR/ASA/SCA/SCAI/SIR/STS/SVM guidelines for the diagnosis and management of patients with Thoracic Aortic Disease: a report of the American College of Cardiology Foundation/American Heart Association Task Force on Practice Guidelines, American Association for Thoracic Surgery, American College of Radiology, American Stroke Association, Society of Cardiovascular Anesthesiologists, Society for Cardiovascular Angiography and Interventions, Society of Interventional Radiology, Society of Thoracic Surgeons, and Society for Vascular Medicine. Circulation 2010;121(13):e266–e369.

75. Gurvitch R, Wood DA, Tay EL, et al. Transcatheter aortic valve implantation: durability of clinical and hemodynamic outcomes beyond 3 years in a large patient cohort. Circulation 2010;122(13):1319–1327.

76. Willson AB, Webb JG, Gurvitch R, et al. Structural integrity of balloon-expandable stents after transcatheter aortic valve replacement: assessment by multidetector computed tomography. JACC Cardiovasc Interv 2012;5(5):525–532.

77. Piazza N, Grube E, Gerckens U, et al. A clinical protocol for analysis of the structural integrity of the Medtronic CoreValve System frame and its application in patients with 1-year minimum follow-up. EuroIntervention 2010;5(6):680–686.